Discover Oncology

Analysis

Actin like 6A is a prognostic biomarker and associated with immune cell infiltration in cancers

Yi He[1] · Ganxun Li[1] · Yu Wu[1] · Ning Cai[1] · Zeyu Chen[1] · Bin Mei[1] · Xiaoping Chen[1] · Bixiang Zhang[1] · Guannan Jin[2] · Zeyang Ding[1]

Received: 17 July 2024 / Accepted: 23 September 2024
Published online: 27 September 2024

Abstract

Purpose To investigate the role of Actin like 6 A (ACTL6A) in cancer and explore the potential mechanism of its function.
Methods Differential expression of ACTL6A was analyzed using Oncomine and TIMER database. Then, we downloaded data sets from TCGA database. The correlation between ACTL6A expression and survival in pan-cancer were analyzed by "survival", "survminer" *R package* and PrognoScan database. STRING (v 11.0) and stringAPP for Cytoscape v3.7.2 were used to predict ACTL6A associated genes. Copy number and methylation alterations of ACTL6A were analyzed using cBioPortal and GSCALite. Transcription factors were downloaded from The Human Transcription Factors Database and analyzed using "limma" *R package*, JASPAR and PROMO database. Correlations analysis between ACTL6A and immune cells were performed using TIMER and GEPIA database.
Results In our studies, we found that ACTL6A was widely upregulated in cancers, which might be attributed to its gene amplifications. Moreover, ACTL6A might regulated by transcription factors (TFs), including E2F1, YY1, CDX2 and HOXD10. In addition, high ACTL6A expression was associated with poor prognosis in most cancers. Meanwhile, ACTL6A was associated with the infiltration of immune cells, especially in liver hepatocellular carcinoma and brain lower grade glioma.
Conclusion Amplification of ACTL6A is correlated with poor prognosis and contribute to immune cells infiltration in LIHC and LGG, which may provide immune-related therapeutic targets to guide clinical strategies.

Keywords Actin like 6A · Pan-cancer · Oncogene · Gene amplification · Immune infiltration

Supplementary Information The online version contains supplementary material available at https://doi.org/10.1007/s12672-024-01388-0.

✉ Guannan Jin, jgnlh@163.com; ✉ Zeyang Ding, zyding@tjh.tjmu.edu.cn; Yi He, heyi8973@163.com; Ganxun Li, ganxunli@hust.edu.cn; Yu Wu, wuyu@tjh.tjmu.edu.cn; Ning Cai, caining0607@126.com; Zeyu Chen, d201981657@hust.edu.cn; Bin Mei, meibingluke@sina.com; Xiaoping Chen, chenxp@tjh.tjmu.edu.cn; Bixiang Zhang, chenxp@tjh.tjmu.edu.cn | [1]Hepatic Surgery Center, Clinical Medicine Research Centre for Hepatic Surgery of Hubei Province, and Hubei Key Laboratory of Hepato-Pancreato-Biliary Diseases, Tongji Hospital, Tongji Medical College, Huazhong University of Science and Technology, No. 1095 Jie Fang Avenue, Wuhan 430030, China. [2]Department of Internal Medicine, Union Hospital, Tongji Medical College, Huazhong University of Science and Technology, No. 1277 Jie Fang Avenue, Wuhan 430000, China.

1 Introduction

Actin-like 6 A (ACTL6A), also known as BAF53A, is a family member of actin-related proteins (ARPs). It encodes a 53-kDa subunit protein of the BAF complex which is functionally related to SWI/SNF complex. In addition, it is also involved in transcriptional regulation, chromatin remodeling and nuclear migration. Recently, ACTL6A was thought to participate in the progress of neural progenitor proliferation, differentiation, and migration during gastrulation [1, 2]. Studies suggested that ACTL6A was highly expressed in long-term repopulating stem cell and contributed to maintaining homeostasis of adults hemopoiesis [3]. Moreover, ACTL6A was proved to be related with poor prognosis of hepatocellular carcinoma (HCC) through promoting epithelia-mesenchymal transition [4]. It also promoted head and neck squamous cell carcinoma (HNSC) by activating YAP signaling pathway [5]. In addition, ACTL6A was found to prevent SWI/SNF complex binding to promoters of KLF4 and other differentiation genes [6]. Another studies found that SWI/SNF might function as tumor suppressor and have effects on immune system [7–9]. Inactivation of SWI/SNF complex was proved to be related with tumor sensitivity to immune checkpoint blockade therapies in solid tumors [10]. However, the role of ACTL6A in pan-cancer and its relationship with immune infiltrating cells have not been illuminated clearly.

Cancers sustained growth, invasion and metastasis in complex tissue environment. There were lots of studies suggesting that the interaction between tumor and the microenvironment was related with tumorigenesis in most cancers. It is known that different tumor microenvironment (TME) forming in each progression step of cancer, has diverse abilities to induce both adverse and beneficial consequences for development of cancers. Recent researches have showed that various types of infiltrating immune cells in TME played multifunctional roles in development of various tumors [11, 12]. Unlike conventional cognize, some of infiltrating immune cells assist tumor cells in surviving from immune system. For example, tumor-associated-macrophages (TAMs) can promote immune escape, tumor angiogenesis and metastasis [13–15]. Tumor-associated neutrophils (TANs) in inflammatory environments recruit macrophages and accelerate progress of tumors [16]. Moreover, infiltrating immune cells, including natural killer cells (NK cells), B cells, CD8+T cells, CD4+T cells, dendritic cells (DC), take part in progression step of tumorigenesis [17]. Immune-related mechanisms indicates potential strategies of immunotherapy for reliable clinical responses [18]. Drugs that target checkpoints, including cytotoxic T lymphocyte-associated antigen 4 (CTLA-4), programmed cell death protein-1 (PD-1) and programmed cell death ligand 1 (PD-L1) have provided survival benefit for many cancer patients [19]. Immunotherapy showed better antitumor effects than chemotherapy in PD-L1 positive non-small-cell lung carcinoma (NSCLC) [20]. Anti-PD-1 antibody combined with locoregional therapy or other molecular targeted agents have been proved to be effective for hepatocellular carcinoma (HCC) [21]. Ipilimumab which blocks CTLA-4 improved overall survival in patients with metastatic melanoma [22]. Thus, there is great significance for discoveries of novel immune-related therapeutic targets to guide clinical strategies.

In this study, we comprehensively analyzed the expression and the prognostic landscape of ACTL6A in pan-cancer using database, including Oncomine, TCGA, PrognoScan, STRING, cBioPortal, JASPAR, PROMO, GSCALite and The Human Transcription Factors Database. The potential relationship between ACTL6A and immune infiltration levels was discovered using TIMER. We found that high expression of ACTL6A in tumor might be driven by its amplifications. Moreover, it was also regulated by transcription factors (TFs), including E2F1, YY1, CDX2 and HOXD10. In addition, it regulated immune cells infiltration and the expression of immune marker sets, which resulted in poorer prognosis in liver hepatocellular carcinoma (LIHC) and brain lower grade glioma (LGG).

2 Methods

2.1 Oncomine database analysis

The mRNA expression of ACTL6A in diverse type cancers was investigated in Oncomine database (https://www.oncomine.org/resource/login.html) [23]. The threshold was adjusted to P value < 0.0001, fold change = 2, and gene rank of top 5%.

2.2 Survival analysis in TCGA and PrognoScan database

The correlation between ACTL6A mRNA expression and survival in different types of cancer was analyzed by "survival", "survminer" *R package* and PrognoScan database (http://www.abren.net/PrognoScan/) [24]. We downloaded data sets

from TCGA database and excluded those data sets (CHOL, DLBC, KICH, UCS) with too few cases. The rest data sets contain 29 types of cancer with 9955 patients' cases. Prognosis of the patients including overall survival (OS), relapse-free survival (RFS), distant metastasis-free survival (DMFS) and distant recurrence free survival (DRFS) were analyzed in PrognoScan database with the threshold adjusted to a Cox *P* value < 0.05.

2.3 Identification of ACTL6A associated genes

Search Tool for the Retrieval of Interacting Genes (STRING) (http://string-db.org/), was used to predict interactive proteins while ACTL6A was input as a query. STRING (v 11.0) is a comprehensive tool providing a profile of all the known and predicted interactions and associations among proteins [25]. The output showed the correlation between different genes, where nodes represent genes and links represent networks with confidence level of 0.90. This result was visualized with stringAPP, a plugin for Cytoscape v3.7.2 (http://www.cytoscape.org/) [26, 27]. Pathway analysis, differential expression analysis and prognostic risk analysis of ACTL6A and associated genes were performed across 33 cancer types using GSCALite database at http://bioinfo.life.hust.edu.cn/web/GSCALite/ [28].

2.4 Complex genomic exploration of ACTL6A

cBioPortal is an open-access resource for investigating genomics data [29]. The database substantially provide high-quality access to molecular view and their clinical attributes, showing accessible interpretation of rich datasets into biologic progress and clinical application. An comprehensive analysis of ACTL6A and clinical features was performed using cBioPortal for Cancer Genomics (http://www.cbioportal.org/index.do). Alterations of the ACTL6A gene was analyzed across available samples ($n = 10967$) in 32 studies. The search parameters contained alterations from GISTIC, including amplifications, deep deletions and missense mutations.

2.5 Copy number variation and methylation analysis

GSCALite is a comprehensive analysis tool for gene set cancer analysis (http://bioinfo.life.hust.edu.cn/web/GSCALite/) [28]. The alterations on DNA or RNA of interested genes may contribute to the cancer initiation, progress, diagnosis, prognosis and therapy [28]. The copy number variation (CNV) and methylation analysis of ACTL6A and associated genes were performed in all 33 cancer types. CNV analysis contained statistics of deletion or amplification of CNV, which was displayed in the form of dots map. Heterozygous and homozygous CNV profile showed percentage of heterozygous CNV, including amplification and deletion percentage of heterozygous CNV about each gene in selected cancers. Only genes with > 5% CNV in cancers will be shown on the figure. The correlation between paired mRNA expression and CNV percent samples was explored, which was based on Person's product moment correlation coefficient, and followed a t distribution. *P*-value was adjusted by FDR. Differential methylation was performed using a student T test to define the methylation difference between tumor tissues and normal tissues. *P* value was adjusted by FDR, FDR < = 0.05 will be considered as significant. Association between paired mRNA expression and methylation was tested, based on Person's product moment correlation coefficient, and follows a t distribution. *P*-value was adjusted by FDR and genes with FDR < = 0.05 will be displayed on the figure. Methylation data and clinical overall survival data was analyzed together. Methylation level of gene was divided into 2 groups by middle level of methylation. Cox regression was performed to estimate the hazards ratio. When Cox coef > 0, the high methylation group shows a poorer survival. The hyper worse was defined as high, otherwise defined as low. Log rank test was also carried out to compare the difference of two groups, *P* value < 0.05 was considered as significant.

2.6 Transcription and analysis

JASPAR (http://jaspar.genereg.net/) is an open-access database of curated, non-redundant transcription factor (TF) binding profiles stored as position frequency matrices (PFMs) and TF flexible models (TFFMs) for TFs [30]. PROMO (http://alggen.lsi.upc.es/cgi-bin/promo_v3/promo/promoinit.cgi?dirDB=TF_8.3) is a virtual laboratory for the exploration of potential transcription factors binding sites (TFBS) in DNA sequences from one species or groups of species [31, 32]. All human transcription factors (TFs) were download from The Human Transcription Factors Database (http://humantfs.ccbr.utoronto.ca/index.php) [33]. Then, co-expression analysis between ACTL6A and TFs was performed using "limma" *R package* across 33 TGCA cancer types. Based on this result, 901 TFs were obtained with the threshold adjusted to *P*

value < 0.05 and cor < − 0.5 or > 0.5 in at least a cancer type. JASPAR and PROMO database were used to predict potential TFs that probably bind to 2 kb upstream or 200 bp downstream of ACTL6A promotor. The intersection of these three groups of TFs, which contained E2F1, YY1, CDX2 and HOXD10, was selected for further analysis. Pathway analysis, differential expression analysis and prognostic risk analysis of ACTL6A and predicted TFs were performed across 33 cancer types using GSCALite database at http://bioinfo.life.hust.edu.cn/web/GSCALite/ [28].

2.7 Correlations analysis between ACTL6A and immune cell in TIMER and GEPIA database

TIMER is a frequently used resource for comprehensive analysis of immune infiltration various type of cancer types (https://cistrome.shinyapps.io/timer/) [34, 35]. The TIMER database containing 10,897 samples across 32 cancer types from The Cancer Genome Atlas (TCGA) is aimed to evaluate the profile of immune cells infiltration. We explored the correlation between ACTL6A expression in diverse types of cancer and the abundance of immune cells infiltration, such as B cells, CD4+T cells, CD8+T cells, neutrophils, macrophages and dendritic cells. The relationship between ACTL6A expression levels and tumor purity was also analyzed in the database. Moreover, correlations between ACTL6A expression and immune markers of tumor-infiltrating immune cells were investigated by correlation modules. The gene markers of tumor-infiltrating immune cells included markers of T cells (general), B cells, monocytes, TAMs, M1 macrophages, M2 macrophages, neutrophils, natural killer (NK) cells, dendritic cells (DCs), T-helper 1 (Th1) cells, T-helper 2 (Th2) cells, follicular helper T (Tfh) cells, T-helper 17 (Th17) cells, Tregs, and exhausted T cells, were obtained from the website of R&D Systems (https://www.rndsystems.com/cn/resources/cell-markers/immune-cells) and previous researches [36–38]. The expression scatter plots were generated by the correlation module with the Spearman's correlation and the estimated statistical significance. The gene expression level was displayed with log2 RSEM. ACTL6A was plotted on x-axis, while marker genes were plotted on y-axis. In addition, correlation analysis of gene expression in GEPIA was performed using TCGA data. The Spearman method was used to identify the correlation coefficient. ACTL6A was plotted on x-axis. Other genes of interest were plotted on y-axis.

2.8 Statistical analysis

Survival curves were generated by the "survival", "survminer" *R package* and PrognoScan database. The results of PrognoScan and GEPIA are displayed with HR and *P* or Cox *P*-values from a log-rank test. The correlation of gene expression was estimated by Spearman's correlation with statistical significance. $P < 0.05$ was considered statistically significant, if not specially noted.

3 Result

3.1 ACTL6A is highly expressed in mRNA level among most human cancers

To explore the mRNA level of ACTL6A in pan-cancer, we analyzed it between tumor and normal tissues using Oncomine in different type of cancers. The result suggested that ACTL6A mRNA was upregulated in tumor tissues compared with adjacent normal tissues in most cancers, including lung cancer, head and neck cancer, brain and CNS cancer, sarcoma, cervical cancer, liver cancer and so on (Fig. 1A). But there was lower expression of ACTL6A in one leukemia dataset and one lymphoma dataset. The detailed results are shown in Supplementary Table 1.

To further reveal the expression of ACTL6A over a cancer-wide range, mRNA sequencing data of ACTL6A in TCGA was analyzed using TIMER. We found that ACTL6A was significantly higher in tumor tissues in digestive system tumors, such as esophageal carcinoma (ESCA), stomach adenocarcinoma (STAD), cholangiocarcinoma (CHOL), liver hepatocellular carcinoma (LIHC), colon adenocarcinoma (COAD), rectum adenocarcinoma (READ), as well as urogenital tumors, such as kidney renal clear cell carcinoma (KIRC), kidney renal papillary cell carcinoma (KIRP), bladder urothelial carcinoma (BLCA), breast invasive carcinoma (BRCA), prostate adenocarcinoma (PRAD), uterine corpus endometrial carcinoma (UCEC), and other tumors, including, head and neck squamous cell carcinoma (HNSC), lung adenocarcinoma (LUAD), lung squamous cell carcinoma (LUSC) (Fig. 1B). In addition, the expression of ACTL6A was higher in tumor tissue of HNSC patients with HPV infection than that without HPV infection. In skin cutaneous melanoma (SKCM), ACTL6A expression was higher in tissues of patients with metastasis. But, in kidney chromophobe (KICH), ACTL6A was lower expressed in tumor tissues. In addition, Immunohistochemistry analyses (https://www.proteinatlas.org) showed that the protein levels of ACTL6A

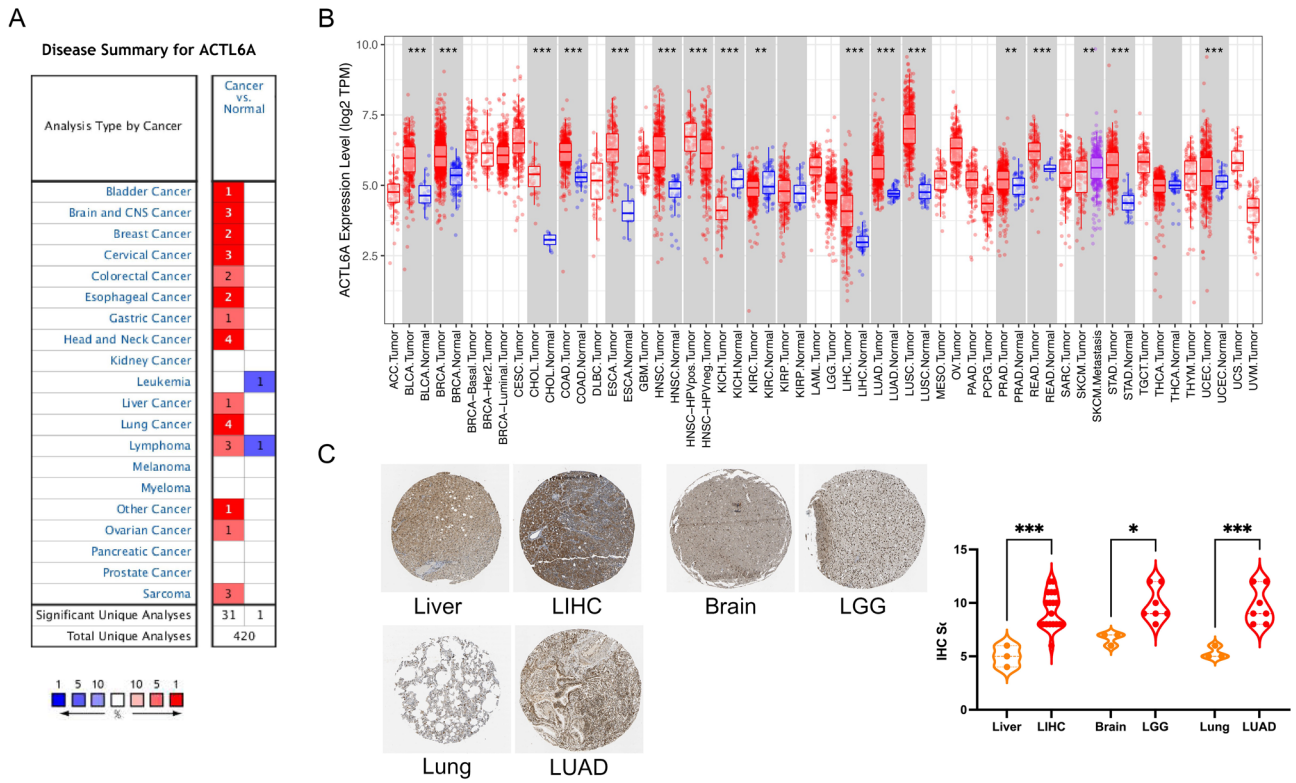

Fig. 1 mRNA expression level of ACTL6A in human cancers. **A** Differential expression of ACTL6A in human cancer data sets compared with normal tissues in Oncomine database. **B** Differential expression of ACTL6A compared with normal tissues were analyzed by TIMER. The data was obtained from TCGA database. **C** Representative IHC staining images of ACTL6A in liver, brain, lung, LIHC, LGG and LUAD tissues obtained from THE HUMAN PROTEIN ATLAS. *$P < 0.05$, **$P < 0.01$, ***$P < 0.001$

were increased in LIHC, LGG and LUAD, compared to normal tissues respectively (Fig. 1C). These results indicated that the expression of ACTL6A was highly expressed in main solid tumor tissues.

3.2 The association of ACTL6A with prognosis in cancers

To investigate whether ACTL6A was correlated with prognosis in diverse cancers patients, we downloaded data sets from TCGA database and excluded those data sets containing too few cases. We investigated the rest of 29 cancer types and found that the expression of ACTL6A had effects on prognosis among 12 type cancers by using "survival" and "survminer" *R package*. High expression of ACTL6A showed significantly poorer overall survival (OS) in 5 type cancers, including ACC (HR = 2.553, 95% CI 1.419 to 4.594, $P = 0.002$), LGG (HR = 2.310, 95% CI 1.576 to 2.878, $P < 0.001$), LIHC (HR = 1.604, 95% CI 1.246 to 2.064, $P < 0.001$), MESO (HR = 1.782, 95% CI 0.988 to 3.215, $P = 0.055$) and PAAD (HR = 3.741, 95% CI 2.080 to 6.793, $P < 0.001$) (Fig. 2A–E and M), but better OS in THCA (HR = 0.693, 95% CI 0.197 to 2.439, $P = 0.568$) and THYM (HR = 0.577, 95% CI 1.019 to 1.768, $P = 0.164$) (Fig. 2F–G and M). In addition, high expression of ACTL6A indicated poorer progression-free survival (PFS) in 5 type cancers, including ACC (HR = 2.118, 95% CI 1.296 to 3.462, $P = 0.003$), LGG (HR = 2.104, 95% CI 1.572 to 2.818, $P < 0.001$), LIHC (HR = 1.354, 95% CI 1.117 to 1.640, $P = 0.002$), PAAD (HR = 2.796, 95% CI 1.614 to 4.845, $P < 0.001$) and SARC (HR = 1.615, 95% CI 1.226 to 2.129, $P < 0.001$) (Fig. 2H–L and N).

To further explore the potential role of ACTL6A in different cancers' prognosis, we used PrognoScan database to estimate the prognostic value of ACTL6A. The detailed results are shown in Supplementary Table 2. High ACTL6A expression suggested poor prognosis for OS in brain cancer (GSE4271-GPL96, HR = 3.09, 95% CI 1.84 to 5.17, $P < 0.001$) (Fig. 3A; Table 1). Three cohorts (GSE12276, GSE12093, GSE2034) included 204 samples, 136 samples and 286 samples of breast cancer indicated that high expression of ACTL6A was associated with poorer prognosis (GSE12276, RFS, HR = 1.92, 95% CI 1.32 to 2.80, $P < 0.001$; GSE12093, DMFS, HR = 13.33, 95% CI 3.16 to 56.11, $P < 0.001$; GSE2034, HR = 2.73, 95% CI 1.71 to 4.38, $P < 0.001$) (Fig. 3B–D; Table 1). In addition, high expression of ACTL6A was also correlated with poor prognosis for lung cancer (GSE13213, HR = 2.58, 95% CI 1.53 to 4.33, $P < 0.001$), skin cancer

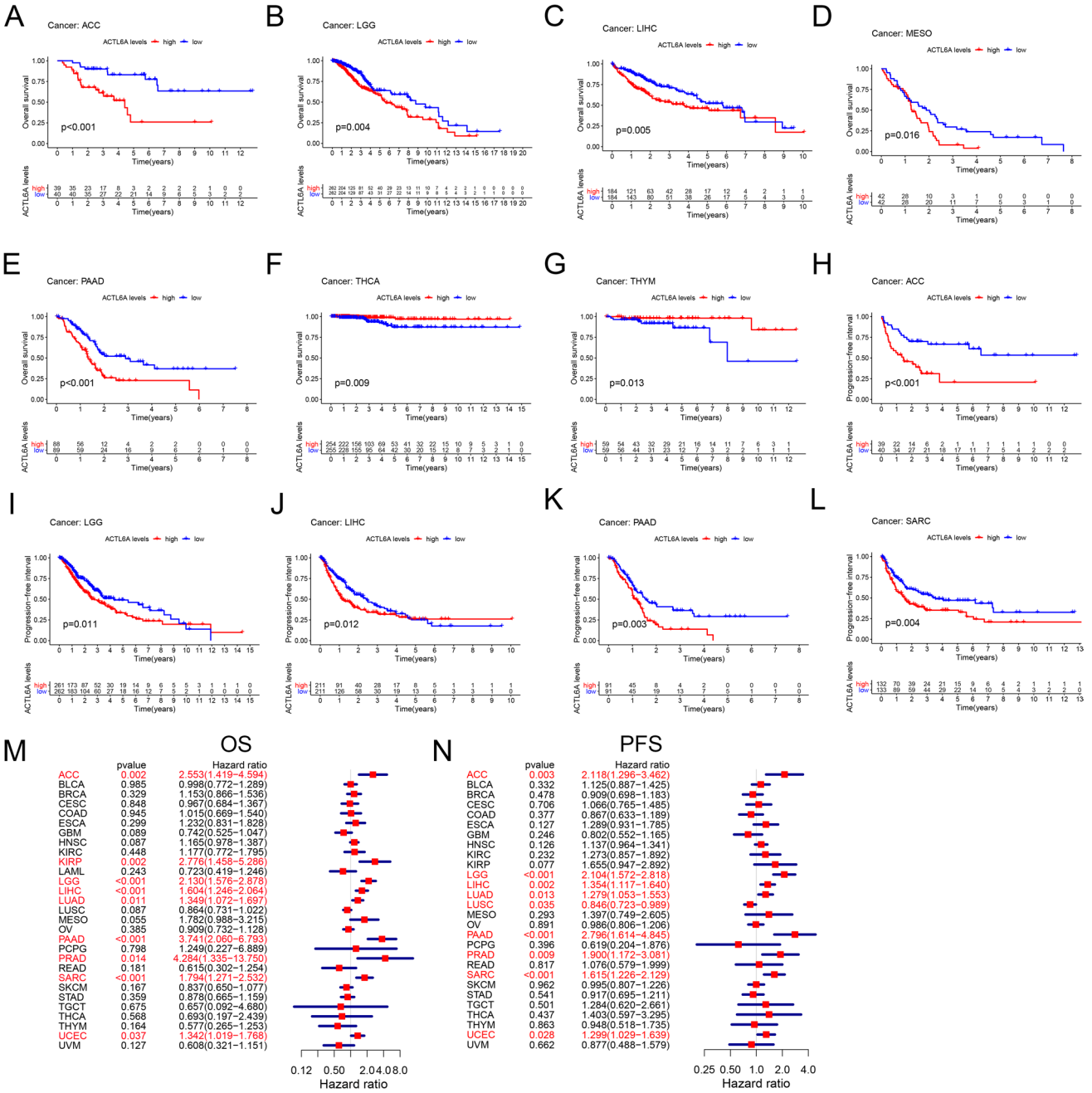

Fig. 2 Prognosis analysis comparing high and low expression of ACTL6A in TCGA cancer types. **A**–**E** High expression of ACTL6A was correlated with poorer prognosis for OS in ACC, LGG, LIHC, MESO, PAAD, **F**, **G** but better prognosis in THCA and THYM. **H**–**L** High expression of ACTL6A was correlated with poorer prognosis for PFS in ACC, LGG, LIHC, PAAD, SARC. **M**, **N** Correlation of ACTL6A mRNA expression with OS and PFS in pan-cancer. Red squares represent hazard ratio. OS: overall survival. PFS: progression free survival

(GSE19234, HR = 6.28, 95% CI 1.81 to 21.84, $P = 0.004$), soft tissue cancer (GSE30929, HR = 2.58, 95% CI 1.43 to 4.65, $P = 0.002$) (Fig. 3E–G; Table 1), but with better prognosis for eye cancer (GSE30929, HR = 0.70, 95% CI 0.50 to 0.98, $P = 0.035$) (Fig. 3H; Table 1).

In summary, these results have suggested that high ACTL6A expression mainly had correlation with poor prognosis in different type cancers.

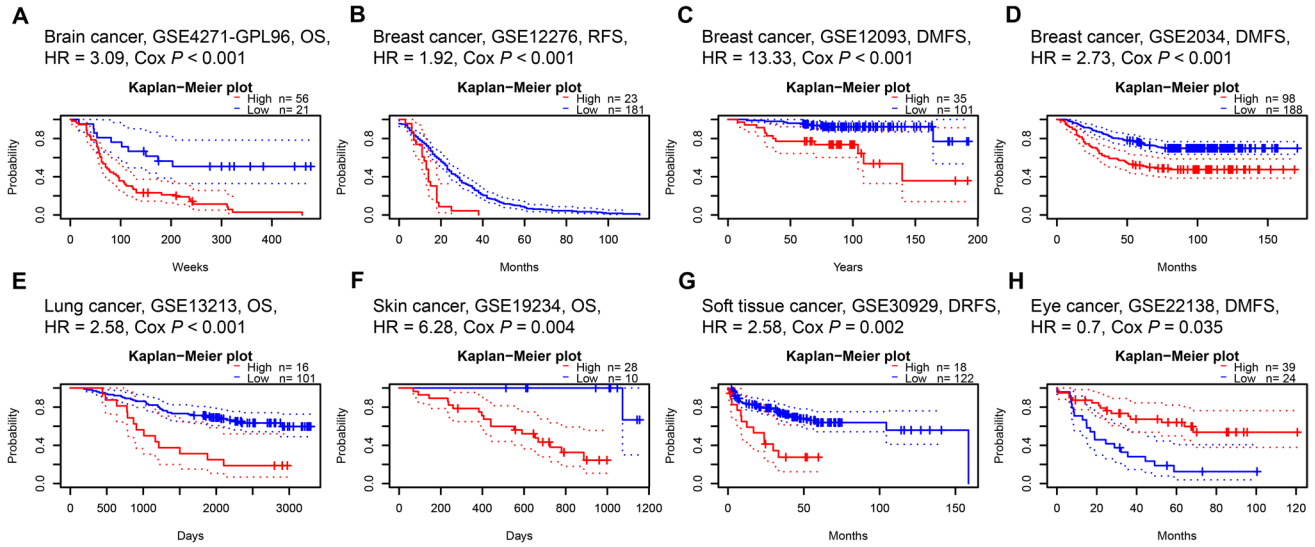

Fig. 3 Kaplan–Meier survival curves comparing the high and low expression of ACTL6A in different types of cancer in PrognoScan. **A** Survival curves of OS in brain cancer cohort [GSE4271-GPL96 ($n=77$)]. **B**–**D** Survival curves of RFS, DMFS in three breast cancer cohorts [GSE12276 ($n=204$), GSE12093 ($n=136$) and GSE2034 ($n=286$)]. **E** Survival curve of OS in lung cancer cohort [GSE13213 ($n=117$)]. **F** Survival curve of OS in skin cancer cohort [GSE19234 ($n=38$)]. **G** Survival curve of DRFS in soft tissue cancer cohort [GSE30929 ($n=140$)]. **H** Survival curve of DMFS in eye cancer cohort [GSE22138 ($n=63$)]. OS: overall survival; RFS: relapse-free survival; DMFS: distant metastasis-free survival; DRFS: distant recurrence free survival

Table 1 Correlation of ACTL6A expression and survival in brain, breast, lung, skin, soft tissue cancer in PrognoScan database

Cancer type	Dataset	Endpoint	*N*	Hazard ratio (95%CI)	CoxP
Brain cancer	GSE4271-GPL96	Overall Survival	77	3.09 [1.84–5.17]	1.85576E−05
Breast cancer	GSE12276	Relapse Free Survival	204	1.92 [1.32–2.80]	0.000672035
Breast cancer	GSE12093	Distant Metastasis Free Survival	136	13.33 [3.16–56.11]	0.000414414
Breast cancer	GSE2034	Distant Metastasis Free Survival	286	2.73 [1.71–4.38]	2.81555E−05
Lung cancer	GSE13213	Overall Survival	117	2.58 [1.53–4.33]	0.000345857
Skin cancer	GSE19234	Overall Survival	38	6.28 [1.81–21.84]	0.00385013
Soft tissue cancer	GSE30929	Distant Recurrence Free Survival	140	2.58 [1.43–4.65]	0.00156948

3.3 Protein–protein interaction network analysis of ACTL6A

ACTL6A is involved in many biological progresses, such as cell proliferation, migration, apoptosis. The analysis of protein–protein interaction (PPI) network is significant to reveal the function of ACTL6A in these progression. Cytoscape stringAPP plugin was used to explore the protein–protein interaction of ACTL6A. Information for PPI prediction was based on curated database, experiment, text-mining, and co-expression/co-occurrence. We found 10 predicted genes correlated with ACTL6A, including transformation/transcription domain associated protein (TRRAP), RuvB like AAA ATPase 1 (RUVBL1), SWI/SNF related, matrix associated, actin dependent regulator of chromatin, subfamily a, member 2 (SMARCA2), SWI/SNF related, matrix associated, actin dependent regulator of chromatin, subfamily a, member 4 (SMARCA4), SWI/SNF related, matrix associated, actin dependent regulator of chromatin subfamily c member 2 (SMARCC2), SWI/SNF related, matrix associated, actin dependent regulator of chromatin subfamily c member 1 (SMARCC1), SWI/SNF related, matrix associated, actin dependent regulator of chromatin, subfamily d, member 1 (SMARCD1), SWI/SNF related, matrix associated, actin dependent regulator of chromatin, subfamily d, member 2 (SMARCD2), SWI/SNF related, matrix associated, actin dependent regulator of chromatin, subfamily b, member 1 (SMARCB1), and SWI/SNF related, matrix associated, actin dependent regulator of chromatin, subfamily e, member 1 (SMARCE1) (Fig. 4A). GSCALite was used to analyze the function of these proteins in cancer pathways. The results showed that most of these predicted genes was related to activation of apoptosis, cell cycle, DNA damage response,

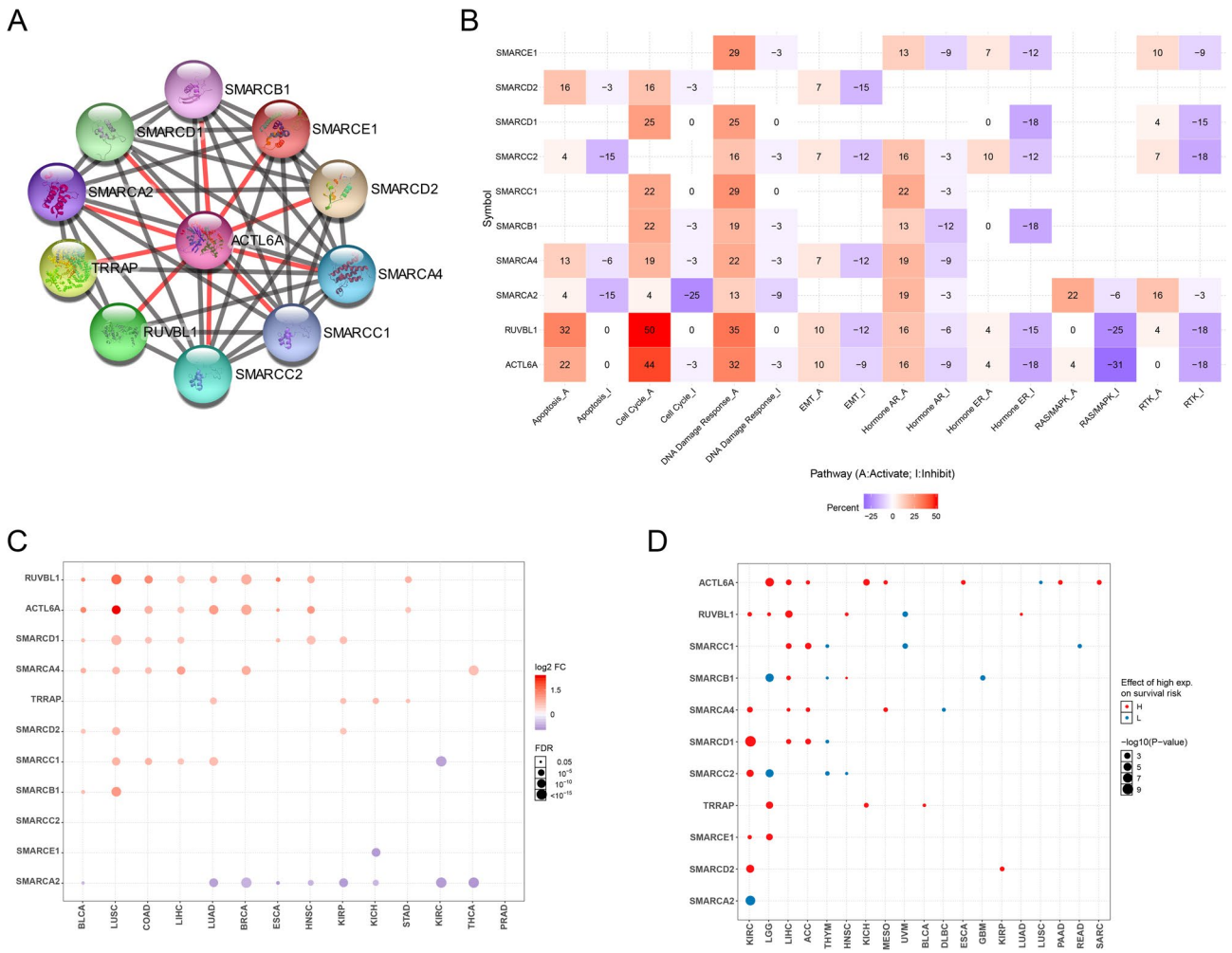

Fig. 4 Genes associated with ACTL6A had effects on different cancers in TCGA. **A** Protein–protein interaction network generated by Cytoscape stringAPP plugin. **B** Heatmap shows indicated genes that have function (activation or inhibition) in at least 7 cancer types. Red suggests activation of the indicated pathway. Blue suggests inhibition of the indicated pathway. **C** Bubble map of the differential expression of ACTL6A and predicted genes between tumor and adjacent tissues. Red dots represent up-regulation in tumor tissues. Blue dots represent down-regulation in tumor tissues, with the deeper the color, the greater the difference. The size of the point represents statistical significance, where the larger the size, the greater the significance. **D** Differential survival of high and low expression of indicated genes in pan-cancer. Genes with p value < 0.05 are shown on the diagram. Red dots indicate worse survival of high expression in tumors, and blue dots indicate the opposite. The sizes of the points represent the statistical significance, where the larger the size, the greater the significance

hormone AR and inhibition of hormone ER, RAS/MAPK, RTK signaling pathway. In addition, ACTL6A and RUVBL1 was associated with activation of cell cycle, DNA damage response and apoptosis in at least 7 cancer types. However, SMARCA2 mainly exhibited inhibition of apoptosis, cell cycle, DNA damage response and activation of RAS/MAPK signaling pathway (Fig. 4B). Then, the differential expression of predicted genes was identified between tumor tissues and adjacent tissues in 33 cancer types. We found that ACTL6A, RUVBL1 and SMARCD1 was upregulated in BLCA, LUSC, COAD, LIHC, ESCA and HNSC. However, SMARCA2 was downregulated in LUAD, BRCA, ESCA, HNSC, KIRP, KIRC and THCA (Fig. 4C). Survival analysis using the Kaplan–Meier method indicated that high expression of predicted genes had higher survival risk in most cancers, specially KIRC, LIHC, LGG and ACC (Fig. 4D). These results confirmed that ACTL6A and associated genes were upregulated and predicted poorer prognosis in LIHC and LGG.

3.4 Overexpression of ACTL6A is associated with amplification in pan-cancer

To find out the mechanisms increasing the expression of ACTL6A and associated genes, we performed genetic alteration analysis using data with 10,967 patients' information from cBioPortal website (www.cbioportal.org/) [29,

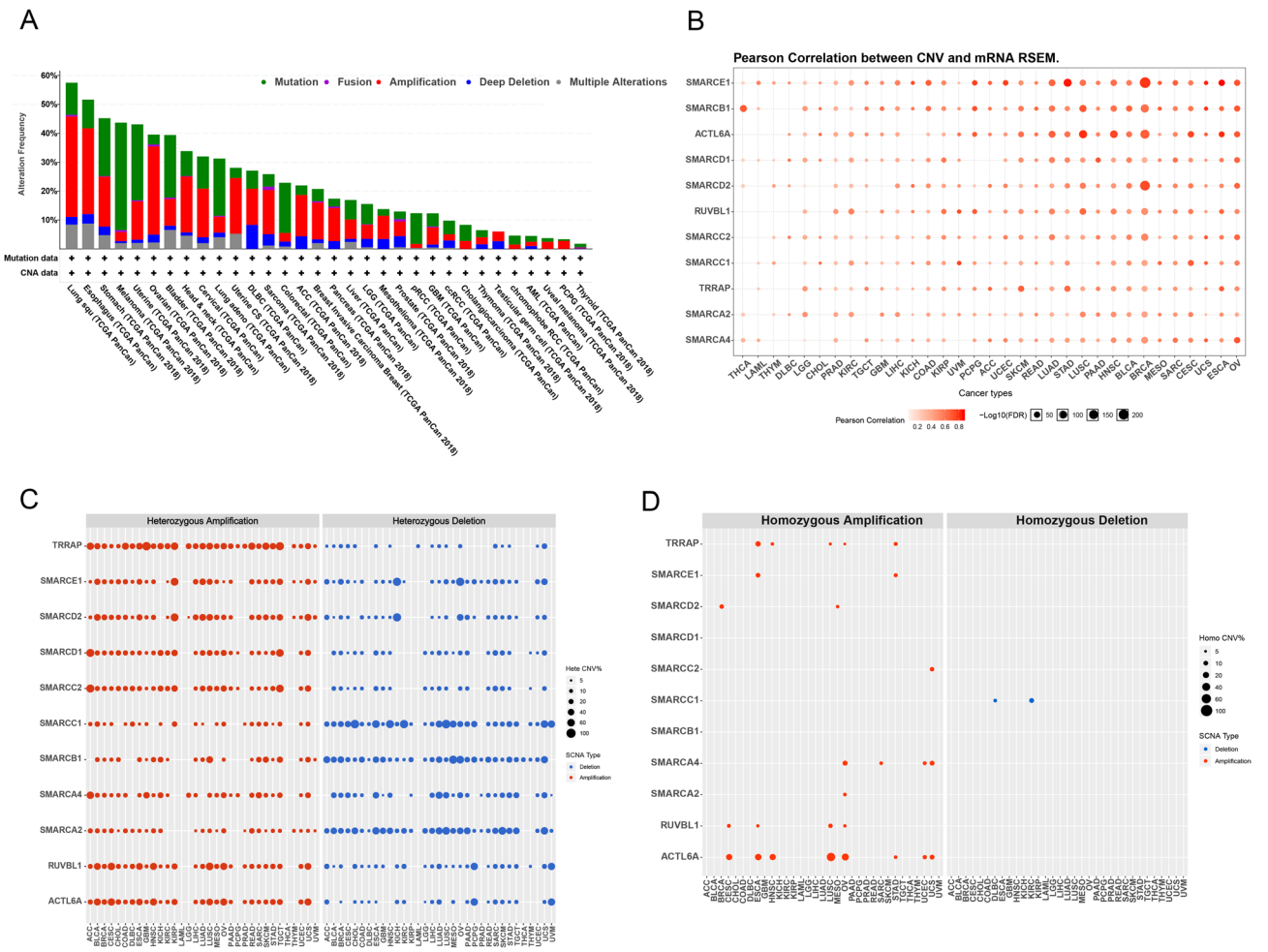

Fig. 5 ACTL6A amplification correlated with the mRNA expression in TCGA pan-cancer. **A** ACTL6A amplification and mutation frequency in TCGA cancer types as determined by GISTIC. **B** Correlation between copy number alteration and mRNA expression of indicated genes in TCGA cancers. Only genes whose mRNA expression significantly (FDR < = 0.05) correlate with CNV were shown on the figure. Red dots represent that copy number positively correlated with mRNA expression in TCGA cancers. The deeper the color, the higher the correlation. The size of the point represents statistical significance, where the larger the size, the greater the significance. **C** Percentage of heterozygous copy number alteration about indicated genes in each cancer. Only genes with > 5% copy number alteration in cancers are shown. Red dots represent heterozygous amplification. Blue dots represent heterozygous deletion. **D** Percentage of homozygous copy number alteration about indicated genes in each cancer. Only genes with > 5% copy number alteration in cancers are shown. Red dots represent homozygous amplification. Blue dots represent homozygous deletion

39]. We identified the frequency of all 11 genes mutation and copy number alteration in 32 cancer types from TCGA (Fig. 5A). High frequency (> 40%) of genetic alteration is observed in LUSC, ESCA, STAD, MESO and uterine cancer. Moreover, we found that amplification was the most common genetic alteration across cancers, especially in OV, LUSC and ESCA. To investigate if all 11 genes copy number was related with their expression, we compared copy number alteration of all 11 genes with their mRNA level in 32 TCGA cancer types. The results indicated a strongly positive correlation between the copy number alteration and mRNA expression in digestive system tumors (ESCA, STAD, CHOL, LIHC, COAD, READ, PAAD), urogenital tumors (KIRP, KIRC, BLCA, PRAD, OV, UCS, CESC, BRCA, UCEC, UVM, TGCT), central nervous system tumors (LGG, GBM) and other tumors (SARC, MESO, LUSC, HNSC, LUAD, SKCM, ACC, PCPG, DLBC) (Fig. 5B). Then, we further explored the amplification and deletion of all 11 genes in pan-cancer. Heterozygous amplification of ACTL6A, RUVBL1, TRRAP had higher ratio compared to heterozygous deletion in in digestive system tumors (CHOL, LIHC, ESCA, PAAD, READ, COAD, STAD), urogenital tumors (BLCA, KICH, KIRC, KIRP, BRCA, CESC, OV, UCEC, UCS, PRAD) and other tumors (ACC, DLBC, GBM, HNSC, LUAD, LUSC, MESO, SARC, SKCM, TGCT) (Fig. 5C). In addition, homozygous amplification of these genes was observed in several cancer types, such as OV, LUSC, ESCA, HNSC, CESC and so on. Homozygous deletion of SMARCC1 was found in DLBC and KIRC (Fig. 5D). These

results confirmed that overexpression of ACTL6A and associated genes was related with amplification in digestive system tumors, urogenital tumors, central nervous system tumors and others.

3.5 Methylation status of ACTL6A in pan-cancer

Methylation of ACTL6A and associated genes were analyzed across 33 TCGA cancer types using GSCALite. We found co-methylation patterns of ACTL6A and associated genes significantly down-regulated in PRAD, BLCA and LUSC (Fig. 6A). However, there was only a little difference of ACTL6A methylation between tumor tissues and adjacent tissues in LUSC, PAAD and HNSC. In addition, the mRNA expression of these genes were negatively correlated with methylation in most TCGA cancer types (Fig. 6B). OS survival analysis was performed to study the difference of survival risk between hypermethylation and hypomethylation. Then, we found that hypermethylation of ACTL6A and associated genes had better prognosis in BRCA, LGG, LIHC, SKCM, UCEC and CESC (Fig. 6C). In addition, hypermethylation of SMARCC1 predicted worse prognosis in GBM, HNSC, LAML, ACC and UVM. These results mentioned above implied limited effects of ACTL6A methylation on the progress of different cancers.

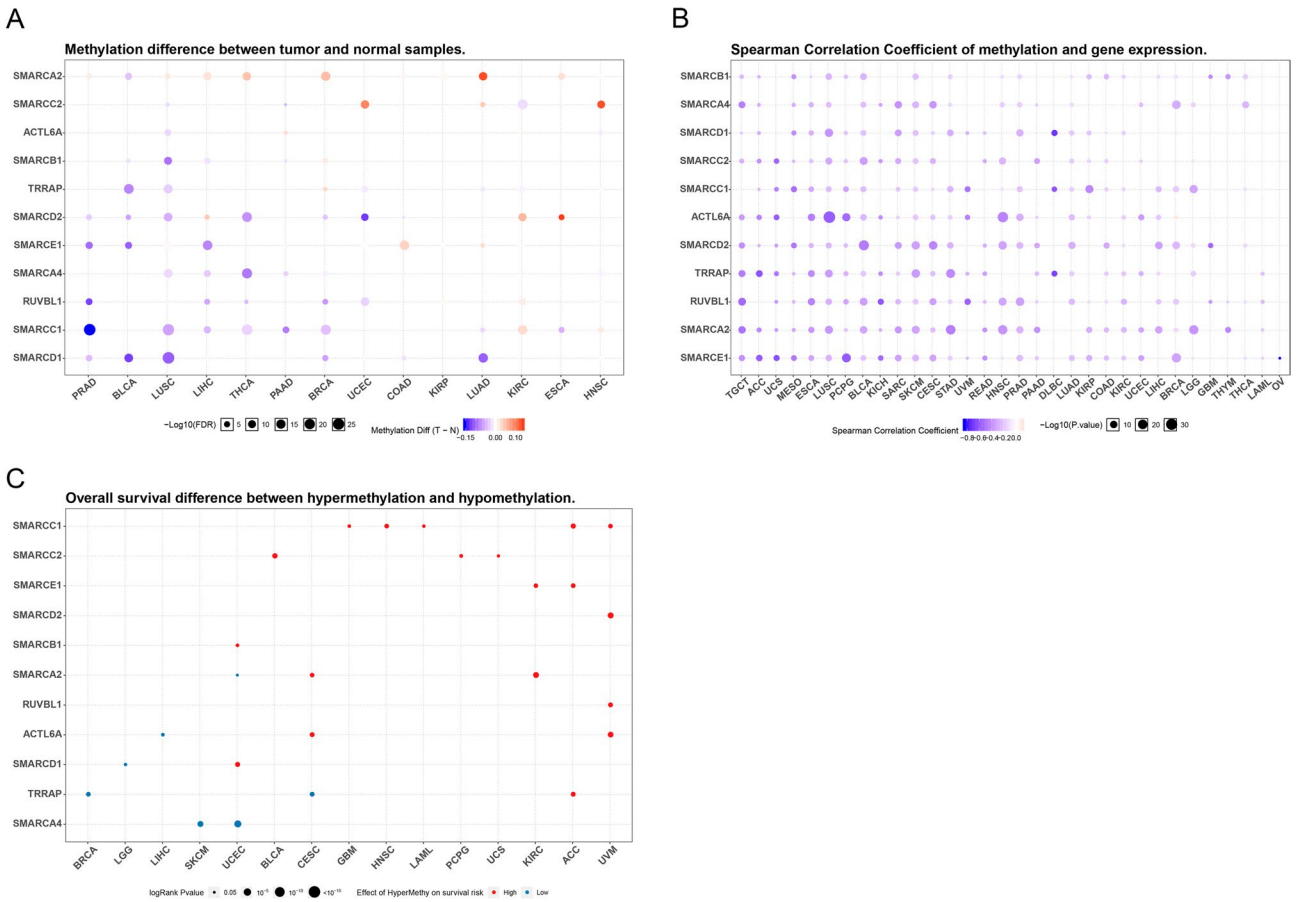

Fig. 6 Methylation and survival analysis of ACTL6A in TCGA cancers. **A** Differential methylation of ACTL6A and associated genes between TCGA cancer and normal samples in pan-cancer. Blue dots represent hypomethylation in tumors, and red dots represent hypermethylation in tumors, with the deeper the color, the greater the difference. The size of the point represents statistical significance, where the larger the size, the greater the significance. **B** Correlation between mRNA expression and methylation of ACTL6A and associated genes in TCGA cancer. Blue dots indicates gene methylation is negatively correlated with mRNA expression. Red dots indicate the opposite. **C** Survival difference between indicated genes' high and low-methylation. Red dots indicate worse survival of high expression in tumors, and blue dots indicate the opposite. The sizes of the points represent the statistical significance, where the larger the size, the greater the significance

3.6 Transcriptional analysis of ACTL6A in pan-cancer

We downloaded all human transcription factors (TFs) in The Human Transcription Factors Database (http://humantfs.ccbr.utoronto.ca/index.php). Then, we obtained 901 TFs significantly (P value < 0.05, cor < − 0.5 or > 0.5) correlated with ACTL6A expression. 126 TFs and 419 TFs were predicted to bound to ACTL6A within 2 kb upstream or 200 downstream of its promoter, using JASPAR and PROMO. Finally, we obtained 4 TFs meeting all requirement above, including E2F1, YY1, CDX2 and HOXD10 (Fig. 7A). E2F1 was suggested to be an oncogene in many cancers, such as gastric cancer [40], BRCA [41, 42], BLCA [43], PRAD [44], LIHC [45] and so on. We found that E2F1 was obviously co-expressed with ACTL6A in LUSC, HNSC, BRCA, LIHC, BLCA, COAD, ESCA, LUAD and STAD (Fig. 7B). Moreover, all these 4 TFs expression were correlated with ACTL6A in LUSC, which probably implied their acceleration of LUSC. Survival analysis of ACTL6A and TFs indicated that both of E2F1 and ACTL6A high expression led to a poorer prognosis in LGG, MESO, KICH and CESC (Fig. 7C). Then, we analyzed the function of ACTL6A and TFs in cancer pathways. ACLT6A and E2F1 expression contributed to activation of apoptosis, cell cycle, DNA damage response pathways, and inhibition of hormone ER, RAS/MAPK, RTK pathways (Fig. 7D), which is similar to the effects of ACTL6A-associated genes

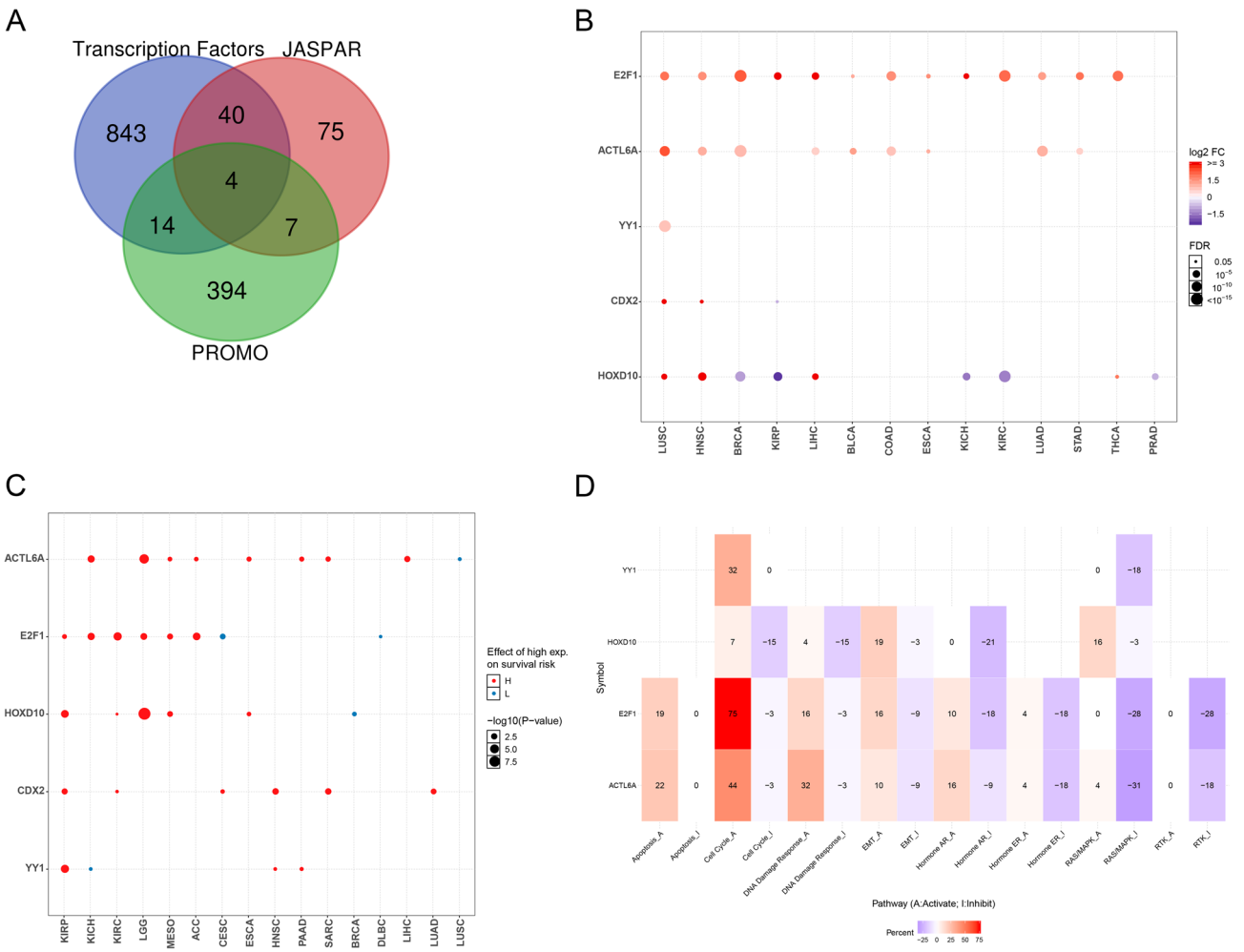

Fig. 7 Co-expression of ACTL6A and TFs in pan-cancer. **A** Venn diagram of the predicted TFs relationship between The Human Transcription Factors Database, JASPAR and PROMO database. **B** Correlation between ACTL6A and predicted TFs in TCGA cancer. The dot was filtered by the fold change (FC > 2) and significance (FDR < 0.05). **C** Differential survival of high and low expression of ACTL6A and predicted TFs in pan-cancer. Genes with p value < 0.05 are shown on the diagram. Red dots indicate worse survival of high expression in tumors, and blue dots indicate the opposite. The sizes of the points represent the statistical significance, where the larger the size, the greater the significance. **D** Heatmap shows ACTL6A and predicted TFs that have function (activation or inhibition) in pan-cancer. Red suggests activation of the indicated pathway. Blue suggests inhibition of the indicated pathway

on signaling pathways (Fig. 4B). Thus, E2F1 might increase the expression of ACTL6A and associated genes to affect these common pathways, which promote the progress of cancers.

3.7 The expression of ACTL6A is related with immune infiltration level in pan-cancer

SWI/SNF was reported to be tumor suppressor through influencing immune system [8]. Meanwhile, ACTL6A inhibited SWI/SNF binding to promoter of KLF4. Thus, we explored if ACTL6A affected immune infiltration in progress of cancers. Correlations of ACTL6A expression with immune infiltration levels were analyzed in 39 cancer types using TIMER. We found that the expression of ACTL6A had significant correlations with tumor purity in 20 cancer types, B cells infiltration levels in 24 cancer types, macrophages infiltration levels in 20 cancer types, neutrophils infiltration levels in 27 cancer types and dendritic cells (DCs) in 20 cancer types. Moreover, expression of ACTL6A was significantly related to CD8+T cells infiltration in 24 cancer types and CD4+T cells infiltration in 18 cancer types (Fig. 8 and Supplementary Fig. 1).

ACTL6A expression had different effects on infiltration level of diverse cancers. In LIHC, expression of ACTL6A positively correlated with immune infiltration levels of B cells (cor = 0.441, $P = 9.01e{-}18$), CD8+T cells (cor = 0.297, $P = 2.18e{-}08$), CD4+T cells (cor = 0.483, $P = 1.65e{-}21$), macrophages (cor = 0.521, $P = 3.83e\text{-}25$), neutrophils (cor = 0.479, $P = 3.25e{-}21$), DCs (cor = 0.457, $P = 5.65e{-}19$) (Fig. 8A). In LGG, expression of ACTL6A positively correlated with immune infiltration levels of B cells (cor = 0.414, $P = 3.46e{-}21$), CD8 + T cells (cor = 0.323, $P = 4.80e{-}13$), CD4+T cells (cor = 0.333, $P = 8.14e{-}14$), macrophages (cor = 0.429, $P = 1.49e{-}22$), neutrophils (cor = 0.298, $P = 3.51e{-}11$), DCs (cor = 0.422, $P = 4.98e{-}22$) (Fig. 8B). Then, we noticed that ACTL6A high expression indicated poorer prognosis in LIHC for OS (HR = 1.604, $P < 0.001$) and PFS (HR = 1.354, $P = 0.002$) (Fig. 2C), in LGG for OS (HR = 2.130, $P < 0.001$) and PFS (HR = 2.104, $P < 0.001$) (Fig. 2B). Thus, ACTL6A probably affected prognosis by influencing immune infiltration level. These results indicated that ACTL6A played important role in immune infiltration in LIHC and LGG.

To further explore the relationship between ACTL6A and immune infiltration, we analyzed immune marker sets of diverse immune cells, including M1 macrophages, M2 macrophages, tumor-associated macrophages (TAMs) and monocytes in LIHC and LGG using TIMER and GEPIA databases. Moreover, the markers of B cells, NK cells, neutrophils, DCs, Th1 cells, Th2 cells, Tfh cells, Th17 cells, Tregs and exhausted T cells were also investigated. After adjusted by tumor purity, the results indicated that ACTL6A expression was significantly related with most immune markers of different immune cells in LIHC and LGG by TIMER database (Supplementary Table 3). To be specific, most markers of monocytes, TAMs, M2 macrophages, including FCGR3A, CD86, CSF1R, CD68, IL10, CD80, CD163, VSIG4 and MS4A4A, were found to be strongly correlated with ACTL6A expression in LIHC (Fig. 8C, D, F) and LGG (Fig. 8G, H, J), which were further confirmed by GEPIA database (Table 2). The expression of ACTL6A was weakly correlated with marker sets of M1 macrophages, such as NOS2, ROS1 (Fig. 8E, I; Table 2 and Supplementary Table 3). Thus, we speculated ACTL6A had significantly correlation with macrophage polarization in LIHC and LGG.

In addition, ACTL6A positively correlated to DCs infiltration level in LIHC and LGG. Moreover, DC markers, such as HLA-DQB1, HLA-DRA, CD1C, NRP1, ITGAX and THBD, had correlation with the expression of ACTL6A (Supplementary Table 3). Also, Treg cell markers showed similar relation with ACTL6A. Expression of ACTL6A was strongly related with the expression of CCR8, STAT5B, TGFB1 and IL2RA. Moreover, the marker sets of T cell exhaustion, including PD-1 (PDCD1), LAG3, HAVCR2, was proved to be correlated with ACTL6A expression. All these results could help to explain how ACTL6A influenced immune cells infiltration and prognosis of cancers.

4 Discussion

ACTL6A is a family member of actin-related proteins (ARPs). Previous studies have revealed the oncogene role of ACTL6A in different cancers [4, 5]. In our study, we found ACTL6A was upregulated in digestive system tumors, such as ESCA, STAD, CHOL, LIHC, COAD, READ, as well as urogenital tumors, such as KIRC, KIRP, BLCA, BRCA, PRAD, UCEC, and other tumors, such as HNSC, LUAD and LUSC (Fig. 1B). To reveal the mechanism of ACTL6A upregulation in tumor tissues, we further explored its genetic and epigenetic variation. In addition, copy number variation (CNV) of ACTL6A has significant correlation with its mRNA expression in digestive system tumors (ESCA, STAD, CHOL, LIHC, COAD, READ, PAAD), urogenital tumors (KIRP, KIRC, BLCA, PRAD, OV, UCS, CESC, BRCA, UCEC, UVM, TGCT), central nervous system tumors (LGG, GBM) and other tumors (SARC, MESO, LUSC, HNSC, LUAD, SKCM, ACC, PCPG, DLBC) (Fig. 5B). Heterozygous amplification of ACTL6A was observed in digestive system tumors (CHOL, LIHC, ESCA, PAAD, READ, COAD, STAD), urogenital tumors (BLCA, KICH, KIRC, KIRP, BRCA, CESC, OV, UCEC, UCS, PRAD) and other tumors (ACC, DLBC, GBM, HNSC, LUAD, LUSC,

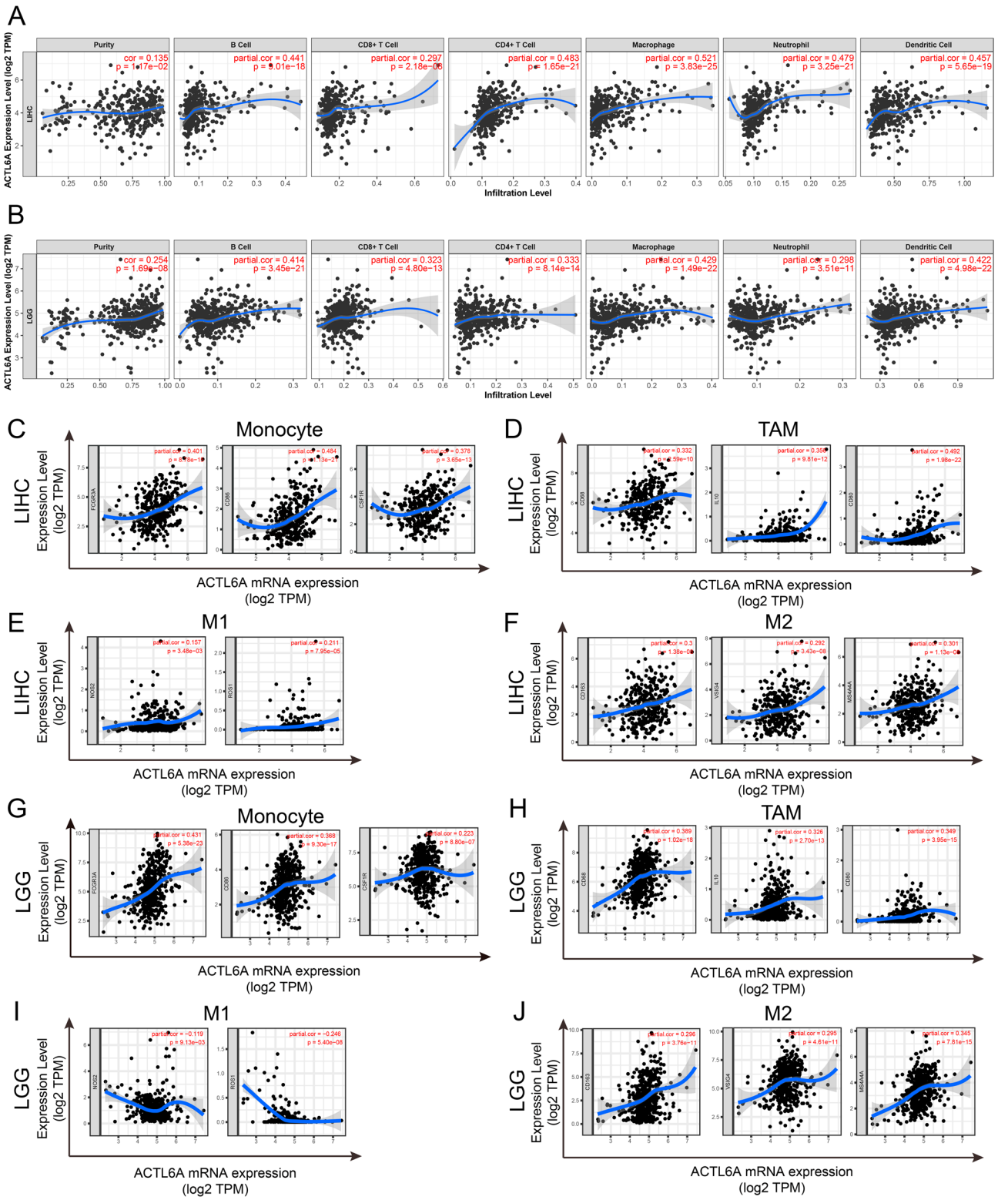

Fig. 8 ACTL6A mRNA expression had positive correlation with infiltration levels in LIHC and LGG. ACTL6A was positive correlated with tumor purity and significantly positive correlated with B cell, CD8+T cell, CD4+T cell, macrophage, neutrophil and dendritic cell **A** in LIHC and **B** in LGG. Markers include FCGR3A, CD86 and CSF1R of monocyte, CD68, IL10 and CD80 of TAM, NOS2 and ROS1 of M1 macrophage, CD163, VSIG4 and MS4A4A of M2 macrophage. **C**–**F** Scatterplots of correlations between ACTL6A expression and gene markers of monocytes (**C**), TAMs (**D**), and M1 (**E**) and M2 macrophages (**F**) in LIHC. **G**–**J** Scatterplots of correlations between ACTL6A expression and gene markers of monocytes (**G**), TAMs (**H**), and M1 (**I**) and M2 macrophages (**J**) in LGG. LIHC: liver hepatocellular carcinoma; LGG: brain lower grade glioma. $P < 0.05$ is considered as significant

Table 2 Correlation of ACTL6A expression and gene markers of immune cells in GEPIA

Cell type		LIHC				LGG	
		Tumor		Normal		Tumor	
		R	P	R	P	R	P
Monocyte	FCGR3A	0.25	***	0.35	0.014	0.25	***
	CD86	0.38	***	0.47	**	0.17	***
	CSF1R	0.28	***	0.41	*	0.057	0.2
TAM	CD68	0.2	***	0.48	**	0.17	**
	IL10	0.36	***	0.32	0.022	0.13	*
	CD80	0.18	**	0.21	0.15	0.16	**
M1 Macrophage	NOS2	0.0015	0.98	0.038	0.79	0.13	*
	ROS1	0.13	0.014	0.12	0.4	−0.26	***
M2 Macrophage	CD163	0.24	***	0.37	*	0.18	***
	VSIG4	0.25	***	0.35	0.013	0.13	*
	MS4A4A	0.24	***	0.44	*	0.14	*

LIHC: Liver hepatocellular carcinoma; LGG: Brain Lower Grade Glioma; TAM: Tumor-associated macrophages. Tumor, co-expression analysis in tumor tissue of TCGA. Normal, co-expression analysis in normal tissue of TCGA. *$P < 0.01$; **$P < 0.001$; ***$P < 0.0001$

MESO, SARC, SKCM, TGCT) (Fig. 5C). Homozygous amplification was also found in CESC, ESCA, LUSC, MESO, OV, STAD, UCEC and UCS (Fig. 5D). Then, we found that methylation of ACTL6A had little differential variation between tumor and normal tissues. Meanwhile, ACTL6A was regulated by several transcription factors (TFs), including E2F1, YY1, CDX2 and HOXD10 (Fig. 7), specially E2F1 which was significantly correlated with ACTL6A mRNA expression in LUSC, HNSC, BRCA, KIRP, BLCA, COAD, ESCA, KICH, KIRC, LUAD, STAD and THCA (Fig. 7). Thus, ACTL6A high expression in tumor might be a result from amplification and was regulated by E2F1.

Previous studies identified the function of ACTL6A in proliferation, invasion and migration [46], suggesting ACTL6A contributed to the progress of cancers. For example, ACTL6A regulated differentiation in acute promyelocytic leukemia cell lines through the Sox2/Notch1 signaling pathway [47]. ACTL6A promotes glioma progression by stabilizing transcriptional regulators YAP/TAZ [48]. In this study, we examined the expression of ACTL6A and prognosis in pan-cancer. We identified ACTL6A was highly expressed in most cancer types, including lung cancer, head and neck cancer, brain and CNS cancer, sarcoma, cervical cancer, liver cancer and so on, using independent datasets in Oncomine and 33 cancer types of TCGA data (Fig. 1A, B). Analysis of TCGA database suggested that high expression of ACTL6A was correlated with poorer prognosis in ACC, LGG, LIHC, MESO, PAAD for OS and PFS (Fig. 2). Moreover, increased ACTL6A expression correlated with high hazard (HR) for poor overall survival (OS) and progress free survival (PFS) of ACC, LGG, LIHC, PAAD, PRAD (Fig. 2M, N). Furthermore, survival analysis of PrognoScan indicated that high level of ACTL6A expression represented poorer prognosis in brain cancer, breast cancer, lung cancer, skin cancer and soft tissue cancer (Fig. 3A–G). These findings indicate that ACTL6A is a biomarker for prognosis in pan-cancer.

Previous studies has shown that ACTL6A prevented SWI/SNF complex from binding to promoters of KLF4 and other differentiation genes [6]. Moreover, SWI/SNF might suppress tumorigenesis and have effects on immune system [7–9]. Inactivation of SWI/SNF complex was correlated with tumor sensitivity to immune checkpoint blockade therapies [10, 49, 50]. So, we continue to explore the role of ACTL6A in immune system during progression of cancer. We found that ACTL6A expression was related with the levels of immune infiltrating cells in cancers. ACTL6A had positive correlation with infiltration levels of B cells, CD8+T cells, CD4+T cells, macrophages, neutrophils and DCs in most cancers, specially LIHC and LGG (Fig. 8A, B and Supplementary Fig. 1). As is reported, CD8+T cells with effective anti-tumor immunity [51] might be suppressed by Tregs, a subset of CD4+T cells [52]. Furthermore, the expression of ACTL6A was significantly correlated with immune cell marker sets expression. We identified ACTL6A was weakly correlated with marker sets of M1 macrophages, such as NOS2, ROS1. Nevertheless, it had strong correlation with marker sets of M2 macrophages, such as CD163, VSIG4, MS4A4A, and marker sets of TAMs, such as CD68, IL10, CD80, in LIHC and LGG (Fig. 8C–J; Table 2 and Supplementary Table 3). These findings have indicated that ACLT6A might play an important role in polarization of tumor-associated macrophages (TAMs), leading to increased M2 macrophages and suppression of anti-tumor immunity [53]. Previous studies has confirmed that dendritic cells (DCs) contributed to tumor metastasis via increasing Treg cells and reducing CD8+T cell cytotoxicity [54]. ACTL6A was related with DCs infiltration and positive correlated marker sets

of infiltrating DCs (Supplementary Table 3). In addition, we also found strong correlation between ACTL6A and Treg and T cell exhaustion marker sets, such as CCR8, STAT5B, TGFB1, IL2RA, PDCD1, LAG3, HAVCR2 (Supplementary Table 3). Besides, monocyte and neutrophils in specific TME were also thought to facilitate formation of the immunosuppressive tumor microenvironment [55, 56]. The positive correlation between ACTL6A and monocyte and neutrophils indicated the progression of tumor. All these results suggested that ACTL6A might promote immune escape, which led to poor prognosis in LIHC and LGG.

Tumor tissues consist of tumor cells, as well as tumor-associated normal epithelial and stromal cells, immune cells and vascular cells. Thus, tumor purity is used to heterogeneity of solid tumor. Previous studied revealed that strong immune cells infiltration always showed low tumor purity [57]. In our study, ACTL6A mainly had positive correlation with tumor purity in various cancers (Fig. 8A, B and Supplementary Fig. 1). Meanwhile, the positive correlation between ACTL6A expression and the infiltration of different immune cells was obvious (Fig. 8 and Supplementary Fig. 1). Then, we noticed lots of studies had revealed that ACTL6A could promote tumor cells proliferation in diverse cancers, including hepatocellular carcinoma (HCC) [4], glioma [58], squamous cell carcinoma [5], ovarian cancer (OV) [59]. We speculated that ACTL6A promoted the proliferation of tumor cells, which increased the level of tumor purity. Thus, we observed positive correlation between ACTL6A expression and tumor purity.

5 Limitations

This study has several limitations. Firstly, most of the information in this study were from microarray or sequencing data, thus there may be a systemic bias introduced during the analysis of immune cell markers at the cellular level. Secondly, this study only focused on bioinformatics analysis of ACTL6A expression and patient prognosis across different databases without validated in vivo/in vitro experiments. Thirdly, we observed the association between ACTL6A expression and immune cell infiltration in tumors, whereas we did not demonstrate a causal relationship in our study. Fourthly, we identified potential heterogeneity of ACTL6A in different tumor tissues, and also found differences in the ways it affects tumor immune infiltration. However, we currently lack the technical means and databases to fully explain this heterogeneity. Fifthly, Although this paper has made a large number of databases to predict the role of ACTL6A in cancer, there is no verification in cell experiments or animal experiments. Prospective studies investigating ACTL6A expression and immune infiltration in tumor patients, and in vitro or in vivo validation experiments may provide more precise answers regarding their relationship in the future.

6 Conclusion

In summary, ACTL6A was upregulated in tumor tissues of most cancers, which probably attributed to its amplification in tumor. In addition, the expression of ACTL6A was also regulated by E2F1, YY1, CDX2 and HOXD10. High expression of ACTL6A correlated with poor prognosis in various cancers. Furthermore, we found ACTL6A might promote infiltration of immune cell, such as B cells, CD8+T cells, CD4+T cells, macrophages, neutrophils, DCs, and correlated with increased immune marker sets, including markers of B cells, NK cells, neutrophils, DCs, Th1 cells, Th2 cells, Tfh cells, Th17 cells, Tregs and exhausted T cells. These results indicated the role of ACTL6A in immune cell infiltration and as a biomarker in pan-cancer.

Acknowledgements We would like to thank all members of hepatic surgery laboratory (Hepatic Surgery Center, Tongji Hospital, Tongji Medical College, Huazhong University of Science and Technology) for continuous assistance throughout this project.

Author contributions Conceptualization, Z.D., G.J., X.C.; Methodology, Y.H., G.L., B.M., X.C., B.Z.; Investigation, Y.H., G.L., Q.G., Y.W. and N.C.; Formal analysis, Z.C., Q.W., Q.S., Z.D. and G.J.; Original draft, Y.H. and G.L. Writing—review and editing, Z.D. and G.J.; Funding acquisition, Z.D.

Funding This work was supported by the National Nature Science Foundation of China (Nos. 82472970, 82273441 and 81874065), National Basic Research Program of China (2020YFA0710700), Knowledge Innovation Program of Wuhan-Shuguang Project (No. 2022020801020456), the first level of the public health youth top talent project of Hubei province (No. 2022SCZ051), and Tongji Hospital (HUST) Foundation for Excellent Young Scientist (Nos. 24-2KYC13057-05 and 2020YQ05).

Data availability The data that support the findings of this study are available from the corresponding author upon reasonable request.

Declarations

Competing interests The authors declare no competing interests.

References

1. Ronan JL, Wu W, Crabtree GR. From neural development to cognition: unexpected roles for chromatin. Nat Rev Genet. 2013;14(5):347–59.
2. Lessard J, Wu JI, Ranish JA, Wan M, Winslow MM, Staahl BT, Wu H, Aebersold R, Graef IA, Crabtree GR. An essential switch in subunit composition of a chromatin remodeling complex during neural development. Neuron. 2007;55(2):201–15.
3. Krasteva V, Buscarlet M, Diaz-Tellez A, Bernard MA, Crabtree GR, Lessard JA. The BAF53a subunit of SWI/SNF-like BAF complexes is essential for hemopoietic stem cell function. Blood. 2012;120(24):4720–32.
4. Xiao S, Chang RM, Yang MY, Lei X, Liu X, Gao WB, Xiao JL, Yang LY. Actin-like 6A predicts poor prognosis of hepatocellular carcinoma and promotes metastasis and epithelial-mesenchymal transition. Hepatology. 2016;63(4):1256–71.
5. Saladi SV, Ross K, Karaayvaz M, Tata PR, Mou H, Rajagopal J, Ramaswamy S, Ellisen LW. ACTL6A is co-amplified with p63 in squamous cell carcinoma to Drive YAP activation, regenerative proliferation, and poor prognosis. Cancer Cell. 2017;31(1):35–49.
6. Bao X, Tang J, Lopez-Pajares V, Tao S, Qu K, Crabtree GR, Khavari PA. ACTL6a enforces the epidermal progenitor state by suppressing SWI/SNF-dependent induction of KLF4. Cell Stem Cell. 2013;12(2):193–203.
7. Reisman D, Glaros S, Thompson EA. The SWI/SNF complex and cancer. Oncogene. 2009;28(14):1653–68.
8. Hu B, Lin JZ, Yang XB, Sang XT. The roles of mutated SWI/SNF complexes in the initiation and development of hepatocellular carcinoma and its regulatory effect on the immune system: a review. Cell Prolif. 2020;53(4):e12791.
9. Panwalkar P, Pratt D, Chung C, Dang D, Le P, Martinez D, Bayliss JM, Smith KS, Adam M, Potter S, et al. SWI/SNF complex heterogeneity relates with polyphenotypic differentiation, prognosis and immune response in rhabdoid tumors. Neuro Oncol. 2020;22(6):785–96.
10. Abou Alaiwi S, Nassar AH, Xie W, Bakouny Z, Berchuck JE, Braun DA, Baca SC, Nuzzo PV, Flippot R, Mouhieddine TH, et al. Mammalian SWI/SNF complex genomic alterations and immune checkpoint blockade in solid tumors. Cancer Immunol Res. 2020;8(8):1075–84.
11. Bindea G, Mlecnik B, Tosolini M, Kirilovsky A, Waldner M, Obenauf AC, Angell H, Fredriksen T, Lafontaine L, Berger A, et al. Spatiotemporal dynamics of intratumoral immune cells reveal the immune landscape in human cancer. Immunity. 2013;39(4):782–95.
12. Quail DF, Joyce JA. Microenvironmental regulation of tumor progression and metastasis. Nat Med. 2013;19(11):1423–37.
13. Mantovani A, Marchesi F, Malesci A, Laghi L, Allavena P. Tumour-associated macrophages as treatment targets in oncology. Nat Rev Clin Oncol. 2017;14(7):399–416.
14. De Palma M, Biziato D, Petrova TV. Microenvironmental regulation of tumour angiogenesis. Nat Rev Cancer. 2017;17(8):457–74.
15. Cully M. Cancer: re-educating tumour-associated macrophages with nanoparticles. Nat Rev Drug Discov. 2018;17(7):468.
16. Kim J, Bae JS. Tumor-associated macrophages and neutrophils in tumor microenvironment. Mediat Inflamm. 2016;2016:6058147.
17. Gajewski TF, Schreiber H, Fu YX. Innate and adaptive immune cells in the tumor microenvironment. Nat Immunol. 2013;14(10):1014–22.
18. Pardoll DM. The blockade of immune checkpoints in cancer immunotherapy. Nat Rev Cancer. 2012;12(4):252–64.
19. Rotte A. Combination of CTLA-4 and PD-1 blockers for treatment of cancer. J Exp Clin Cancer Res. 2019;38(1):255.
20. Reck M, Rodriguez-Abreu D, Robinson AG, Hui R, Csoszi T, Fulop A, Gottfried M, Peled N, Tafreshi A, Cuffe S, et al. Pembrolizumab versus chemotherapy for PD-L1-positive non-small-cell lung cancer. N Engl J Med. 2016;375(19):1823–33.
21. Xu F, Jin T, Zhu Y, Dai C. Immune checkpoint therapy in liver cancer. J Exp Clin Cancer Res. 2018;37(1):110.
22. Hodi FS, O'Day SJ, McDermott DF, Weber RW, Sosman JA, Haanen JB, Gonzalez R, Robert C, Schadendorf D, Hassel JC, et al. Improved survival with ipilimumab in patients with metastatic melanoma. N Engl J Med. 2010;363(8):711–23.
23. Rhodes DR, Kalyana-Sundaram S, Mahavisno V, Varambally R, Yu J, Briggs BB, Barrette TR, Anstet MJ, Kincead-Beal C, Kulkarni P, et al. Oncomine 3.0: genes, pathways, and networks in a collection of 18,000 cancer gene expression profiles. Neoplasia. 2007;9(2):166–80.
24. Mizuno H, Kitada K, Nakai K, Sarai A. PrognoScan: a new database for meta-analysis of the prognostic value of genes. BMC Med Genomics. 2009;2:18.
25. Franceschini A, Szklarczyk D, Frankild S, Kuhn M, Simonovic M, Roth A, Lin J, Minguez P, Bork P, von Mering C, et al. STRING v9.1: protein-protein interaction networks, with increased coverage and integration. Nucleic Acids Res. 2013;41(Database issue):D808–15.
26. Saito R, Smoot ME, Ono K, Ruscheinski J, Wang P-L, Lotia S, Pico AR, Bader GD, Ideker T. A travel guide to Cytoscape plugins. Nat Methods. 2012;9(11):1069–76.
27. Doncheva NT, Morris JH, Gorodkin J, Jensen LJ. Cytoscape StringApp: network analysis and visualization of proteomics data. J Proteome Res. 2019;18(2):623–32.
28. Liu C-J, Hu F-F, Xia M-X, Han L, Zhang Q, Guo A-Y. GSCALite: a web server for gene set cancer analysis. Bioinformatics. 2018;34(21):3771–2.
29. Cerami E, Gao J, Dogrusoz U, Gross BE, Sumer SO, Aksoy BA, Jacobsen A, Byrne CJ, Heuer ML, Larsson E, et al. The cBio cancer genomics portal: an open platform for exploring multidimensional cancer genomics data. Cancer Discov. 2012;2(5):401–4.

30. Fornes O, Castro-Mondragon JA, Khan A, van der Lee R, Zhang X, Richmond PA, Modi BP, Correard S, Gheorghe M, Baranašić D, et al. JASPAR 2020: update of the open-access database of transcription factor binding profiles. Nucleic Acids Res. 2020;48(D1):D87–92.
31. Messeguer X, Escudero R, Farré D, Núñez O, Martínez J, Albà MM. PROMO: detection of known transcription regulatory elements using species-tailored searches. Bioinformatics. 2002;18(2):333–4.
32. Farré D, Roset R, Huerta M, Adsuara JE, Roselló L, Albà MM, Messeguer X. Identification of patterns in biological sequences at the ALGGEN server: PROMO and MALGEN. Nucleic Acids Res. 2003;31(13):3651–3.
33. Lambert SA, Jolma A, Campitelli LF, Das PK, Yin Y, Albu M, Chen X, Taipale J, Hughes TR, Weirauch MT. The human transcription factors. Cell. 2018;172(4):650–65.
34. Li T, Fan J, Wang B, Traugh N, Chen Q, Liu JS, Li B, Liu XS. TIMER: a web server for comprehensive analysis of tumor-infiltrating immune cells. Cancer Res. 2017;77(21):e108-10.
35. Li B, Severson E, Pignon J-C, Zhao H, Li T, Novak J, Jiang P, Shen H, Aster JC, Rodig S, et al. Comprehensive analyses of tumor immunity: implications for cancer immunotherapy. Genome Biol. 2016;17(1):174.
36. Siemers NO, Holloway JL, Chang H, Chasalow SD, Ross-MacDonald PB, Voliva CF, Szustakowski JD. Genome-wide association analysis identifies genetic correlates of immune infiltrates in solid tumors. PLoS ONE. 2017;12(7):e0179726.
37. Danaher P, Warren S, Dennis L, D'Amico L, White A, Disis ML, Geller MA, Odunsi K, Beechem J, Fling SP. Gene expression markers of tumor infiltrating leukocytes. J Immunother Cancer. 2017;5:18.
38. Sousa S, Määttä J. The role of tumour-associated macrophages in bone metastasis. J Bone Oncol. 2016;5(3):135–8.
39. Gao J, Aksoy BA, Dogrusoz U, Dresdner G, Gross B, Sumer SO, Sun Y, Jacobsen A, Sinha R, Larsson E, et al. Integrative analysis of complex cancer genomics and clinical profiles using the cBioPortal. Sci Signal. 2013;6(269):pl1.
40. Xu TP, Wang YF, Xiong WL, Ma P, Wang WY, Chen WM, Huang MD, Xia R, Wang R, Zhang EB, et al. E2F1 induces TINCR transcriptional activity and accelerates gastric cancer progression via activation of TINCR/STAU1/CDKN2B signaling axis. Cell Death Dis. 2017;8(6):e2837.
41. Hollern DP, Swiatnicki MR, Rennhack JP, Misek SA, Matson BC, McAuliff A, Gallo KA, Caron KM, Andrechek ER. E2F1 drives breast cancer metastasis by regulating the target gene FGF13 and altering cell migration. Sci Rep. 2019;9(1):10718.
42. Zheng X, Huang M, Xing L, Yang R, Wang X, Jiang R, Zhang L, Chen J. The circRNA circSEPT9 mediated by E2F1 and EIF4A3 facilitates the carcinogenesis and development of triple-negative breast cancer. Mol Cancer. 2020;19(1):73.
43. Lee SR, Roh YG, Kim SK, Lee JS, Seol SY, Lee HH, Kim WT, Kim WJ, Heo J, Cha HJ, et al. Activation of EZH2 and SUZ12 regulated by E2F1 predicts the disease progression and aggressive characteristics of bladder Cancer. Clin Cancer Res. 2015;21(23):5391–403.
44. Rodriguez-Bravo V, Pippa R, Song WM, Carceles-Cordon M, Dominguez-Andres A, Fujiwara N, Woo J, Koh AP, Ertel A, Lokareddy RK, et al. Nuclear pores promote lethal prostate cancer by increasing POM121-Driven E2F1, MYC, and AR nuclear import. Cell. 2018;174(5):1200–e12151220.
45. Gu Y, Wang X, Liu H, Li G, Yu W, Ma Q. SET7/9 promotes hepatocellular carcinoma progression through regulation of E2F1. Oncol Rep. 2018;40(4):1863–74.
46. Wee Y, Liu Y, Lu J, Li X, Zhao M. Identification of novel prognosis-related genes associated with cancer using integrative network analysis. Sci Rep. 2018;8(1):3233.
47. Zhong P-Q, Zhong L, Yao J-J, Liu D-D, Yuan Z, Liu J-M, Chen M, Yao S-F, Zhao Y, Liu L, et al. ACTL6A interacts with p53 in acute promyelocytic leukemia cell lines to affect differentiation via the Sox2/Notch1 signaling pathway. Cell Signal. 2019;53:390–9.
48. Ji J, Xu R, Zhang X, Han M, Xu Y, Wei Y, Ding K, Wang S, Bin H, Chen A, et al. Actin like-6A promotes glioma progression through stabilization of transcriptional regulators YAP/TAZ. Cell Death Dis. 2018;9(5):517.
49. Miao D, Margolis CA, Gao W, Voss MH, Li W, Martini DJ, Norton C, Bossé D, Wankowicz SM, Cullen D, et al. Genomic correlates of response to immune checkpoint therapies in clear cell renal cell carcinoma. Science. 2018;359(6377):801–6.
50. Mittal P, Roberts CWM. The SWI/SNF complex in cancer - biology, biomarkers and therapy. Nat Rev Clin Oncol. 2020;17(7):435–48.
51. Ozga AJ, Chow MT, Luster AD. Chemokines and the immune response to cancer. Immunity. 2021;54(5):859–74.
52. Tanaka A, Sakaguchi S. Regulatory T cells in cancer immunotherapy. Cell Res. 2017;27(1):109–18.
53. Yunna C, Mengru H, Lei W, Weidong C. Macrophage M1/M2 polarization. Eur J Pharmacol. 2020;877:173090.
54. Sawant A, Hensel JA, Chanda D, Harris BA, Siegal GP, Maheshwari A, Ponnazhagan S. Depletion of plasmacytoid dendritic cells inhibits tumor growth and prevents bone metastasis of breast cancer cells. J Immunol. 2012;189(9):4258–65.
55. Ugel S, Canè S, De Sanctis F, Bronte V. Monocytes in the tumor microenvironment. Annu Rev Pathol. 2021;16:93–122.
56. Que H, Fu Q, Lan T, Tian X, Wei X. Tumor-associated neutrophils and neutrophil-targeted cancer therapies. Biochim Biophys Acta Rev Cancer. 2022;1877(5):188762.
57. Yoshihara K, Shahmoradgoli M, Martínez E, Vegesna R, Kim H, Torres-Garcia W, Treviño V, Shen H, Laird PW, Levine DA, et al. Inferring tumour purity and stromal and immune cell admixture from expression data. Nat Commun. 2013;4:2612.
58. Meng L, Wang X, Liao W, Liu J, Liao Y, He Q. BAF53a is a potential prognostic biomarker and promotes invasion and epithelial-mesenchymal transition of glioma cells. Oncol Rep. 2017;38(6):3327–34.
59. Zhang J, Zhang J, Wei Y, Li Q, Wang Q. ACTL6A regulates follicle-stimulating hormone-driven glycolysis in ovarian cancer cells via PGK1. Cell Death Dis. 2019;10(11):811.